

# New Regime of MHD Turbulence: Cascade Below Viscous Cutoff

Jungyeon Cho & Alex Lazarian

*Dept. of Astronomy, University of Wisconsin, 475 N. Charter St., Madison, WI53706;*  
*cho, lazarian@astro.wisc.edu*

Ethan T. Vishniac

*Dept. of Physics and Astronomy, Johns Hopkins University, 3400 N. Charles St.,  
Baltimore, MD 21218; ethan@pha.jhu.edu*

## ABSTRACT

In astrophysical situations, e.g. in the interstellar medium (ISM), neutrals can provide viscous damping on scales much larger than the magnetic diffusion scale. Through numerical simulations, we have found that the magnetic field can have a rich structure below the dissipation cutoff scale. This implies that magnetic fields in the ISM can have structures on scales much smaller than parsec scales. Our results show that the magnetic energy contained in a wavenumber band is independent of the wavenumber and magnetic structures are intermittent and extremely anisotropic. We discuss the relation between our results and the formation of the tiny-scale atomic structure (TSAS).

*Subject headings:* ISM:general—ISM:structure—MHD—turbulence

## 1. Introduction

In the interstellar medium (ISM), flows are complicated and dynamic. Observations suggest that the ISM is in a turbulent state (Larson 1981; Myers 1983; Scalo 1984; Armstrong, Rickett & Spangler 1995; Stanimirovic & Lazarian 2001).

Hydrodynamic turbulence can be described by so-called energy cascade model, in which energy injected at a scale  $L$  cascades down to progressively smaller and smaller scales. Ultimately, the energy will reach the molecular *dissipation scale*  $l_d$  and the energy will be lost there. The scales between  $L$  and  $l_d$  constitute the *inertial range*. In hydrodynamic turbulence the dissipation scale is the minimal scale for motion. If we plot kinetic energy spectrum  $E_v(k)$ , the kinetic energy contained in a wavenumber band, we will see that a) the spectrum peaks at the wavenumber corresponding to the energy injection scale ( $k_L \sim 1/L$ );

b) it follows a power law (e.g.  $E_v(k) \propto k^{-5/3}$  in Kolmogorov theory) in the inertial range; c) it drops rapidly after  $k_d \sim 1/l_d$ , which depends on viscosity  $\nu$ :  $k_d \sim (VL/\nu)^{3/4}k_L$ , where  $V$  is the rms velocity at the energy injection scale  $L$ .

Magnetohydrodynamic (MHD) turbulence has two energy loss scales - a viscous damping scale set by the viscosity  $\nu$  and magnetic diffusion scale set by the ohmic resistivity  $\eta$ . When  $\nu \gg \eta$ , the viscous damping scale is much larger than the magnetic diffusion scale. Although MHD turbulence is different from its hydrodynamic counterpart in many ways, the energy cascade model is still valid (e.g. Goldreich & Sridhar 1995). Therefore, in this case, kinetic energy is damped before the cascading energy reaches the magnetic diffusion scale. In this paper we study MHD turbulence when the mean field  $B_0$  is at least as large as the fluctuating field  $b$ . This is the opposite of the dynamo regime with  $B_0 \ll b$  discussed in Kulsrud & Anderson (1992) and tested in Maron & Cowley (2001). We shall show that the wide-spread assumption that magnetic structures do not exist below the viscous cutoff is wrong.

In astrophysics, the viscosity caused by neutrals damps turbulence. In the ISM, this viscous cutoff occurs at  $\sim pc$  scales, which is much larger than the magnetic diffusion scale. To model this, we use a large physical viscosity and very small magnetic diffusivity.

In this letter we numerically demonstrate the existence of a power-law magnetic energy spectrum below the viscous damping scale. We use an incompressible MHD code.

## 2. Method

**Numerical Method.** We have calculated the time evolution of incompressible magnetic turbulence subject to a random driving force per unit mass. We have adopted a pseudo-spectral code to solve the incompressible MHD equations in a periodic box of size  $2\pi$  (see more in Lazarian, Vishniac & Cho 2002):

$$\frac{\partial \mathbf{v}}{\partial t} = -(\nabla \times \mathbf{v}) \times \mathbf{v} + (\nabla \times \mathbf{B}) \times \mathbf{B} + \nu \nabla^2 \mathbf{v} + \mathbf{f} + \nabla P', \quad (1)$$

$$\frac{\partial \mathbf{B}}{\partial t} = \nabla \times (\mathbf{v} \times \mathbf{B}) + \eta \nabla^2 \mathbf{B}, \quad (2)$$

where  $\mathbf{f}$  is a random driving force,  $P' \equiv P/\rho + v^2/2$ ,  $\mathbf{v}$  is the velocity, and  $\mathbf{B}$  is magnetic field divided by  $(4\pi\rho)^{1/2}$ . In this representation,  $\mathbf{v}$  can be viewed as the velocity measured in units of the rms velocity of the system and  $\mathbf{B}$  as the Alfvén speed in the same units. The time  $t$  is in units of the large eddy turnover time ( $\sim L/V$ ) and the length in units of  $L$ , the scale of the energy injection. In this system of units, the viscosity  $\nu$  and magnetic diffusivity  $\eta$  are the inverse of the kinetic and magnetic Reynolds numbers respectively. The magnetic

field consists of the uniform background field and a fluctuating field:  $\mathbf{B} = \mathbf{B}_0 + \mathbf{b}$ . The Alfvén speed of the background field,  $B_0$ , is set to 1. We use the same numerical technique as in Cho & Vishniac (2000).

We use a physical viscosity ( $\nu = 0.015$ ) and hyper diffusion. The power of hyperdiffusion is set to 2 or 3, so that the magnetic dissipation term in the above equation is replaced with  $-\eta_n(\nabla^2)^n \mathbf{v}$ , where  $n = 2$  or  $3$  and  $\eta_n$  ( $=\eta_2$  or  $\eta_3$ ) is adjusted in such a way that the magnetic dissipation occurs around  $k \sim N/3$ , where  $N$  is the number of grids in each spatial direction. This way, we can avoid the aliasing error of the pseudo-spectral method. We use the notation 384XY- $B_0$ Z, where 384 refers to the number of grid points in each spatial direction; X=P refers to physical viscosity; Y = H2, H3 refers to hyper-diffusion (and its power); Z=1 refers to the strength of the external magnetic field.

**Parameter Space.** We require that the Alfvén frequency is similar to the eddy turnover rate at the energy injection scale:  $B_0 k_{\parallel,L} \approx V k_{\perp,L}$ , where  $k_{\parallel,L}$  and  $k_{\perp,L}$  are the wavenumbers parallel and perpendicular to  $\mathbf{B}_0$  at the scale, respectively. We require a large viscosity to maximize the dynamical range of the damped, conducting regime, but we need  $\nu$  small enough to guarantee large scale turbulence. Therefore, we take  $\nu \sim 0.015$  (for a Reynolds number  $R \equiv LV/\nu \sim 100$ ). When we take  $\nu = 0.015$ ,  $k_L \sim 2.5$ , and  $V \sim 0.6$ , then  $k_d \equiv R^{3/4} k_L \sim 70$ . In practice, the kinetic energy spectrum usually begins to drops rapidly one decade before  $k_d$ , so the viscous cutoff scale is around  $k = 7$ . We also require  $\nu \gg \eta$ . Therefore, we take hyper-diffusion for magnetic field. We consider only low order hyper-diffusion. Using hyper-diffusion, we can have a very small magnetic diffusion for small  $k$ 's and very strong diffusion at large  $k$ 's so that the large scale magnetic field is largely unaffected by ohmic dissipation.

### 3. Results

**Time Evolution and Spectra.** About 4 to 5 time units after the start of the simulation, the system has reached a statistically stationary state, where the average rms velocity ( $\sim 0.6$ ) is roughly equal to the average strength of the random magnetic field. Energy spectra reach a statistically stationary state a bit later at  $\sim 6$ . For the run 384PH2-B<sub>0</sub>1 we integrate the MHD equations from  $t = 0$  to  $t = 12$ . For the run 384PH3-B<sub>0</sub>1 we integrate the MHD equations from  $t = 8$  to  $t = 12$ , where we use a data cube from the run 384PH2-B<sub>0</sub>1 at  $t = 8$  as the input. We calculate energy spectra and other quantities at  $t \sim 12$ .

In Figure 1, we plot energy spectra at  $t=12$ . The spectra consist of several parts. First, the peak of the spectra corresponds to the energy injection scale. Second, for  $2 < k < 7$ ,

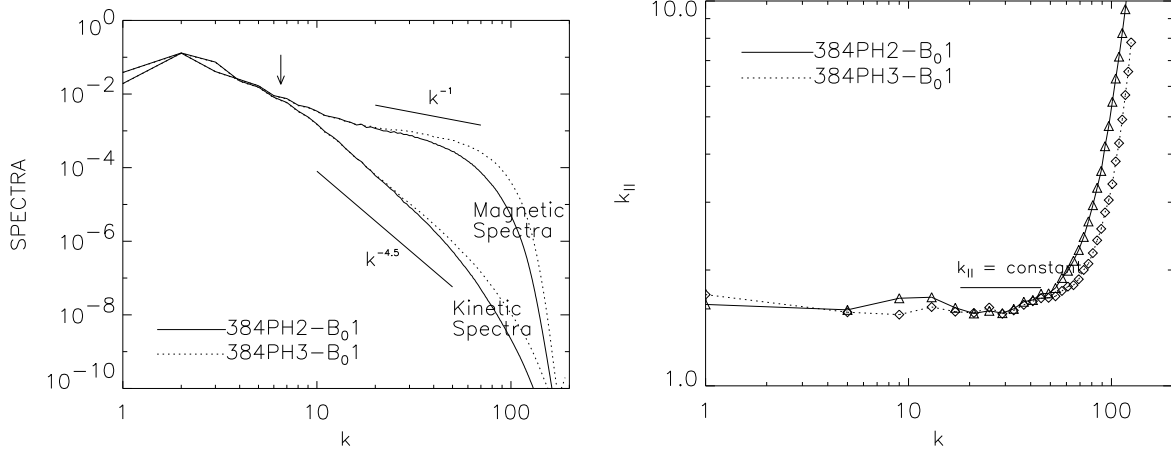


Fig. 1.— Energy spectra  $E_v(k)$  and  $E_b(k)$  at  $t=12$ . Spectra of 384PH2- $B_01$  and 384PH3- $B_01$  almost exactly coincide at small wavenumbers. Run 384PH3- $B_01$  has more extended inertial range below the viscous cutoff (marked by an arrow).

Fig. 2.— Parallel wavenumber  $k_{\parallel}$ . Solid line: 384PH2- $B_01$  at  $t=10$ . Dotted line: 384PH3- $B_01$  at  $t=12$ .

kinetic and magnetic spectra follow a similar slope. This part is more or less a severely truncated inertial range for undamped MHD turbulence. Third, the magnetic and kinetic spectra begin to decouple at  $k \sim 7$ . Fourth, after  $k \sim 20$ , a new damped-scale inertial range emerges. We checked that the tail of the magnetic fluctuations is a real physical effect and not due to a bottle-neck, by comparing with calculations with a real magnetic diffusivity and obtaining a similar effect.

In summary, scaling for energy spectra *below the viscous cutoff* is as follows. The magnetic spectrum from Run 384PH2- $B_01$  follows

$$E_b(k) \propto k^{-1}. \quad (3)$$

while Run 384PH3- $B_01$  shows a slightly shallower slope. The kinetic energy spectra are roughly

$$E_v(k) \propto k^{-4.5}. \quad (4)$$

**Scaling of  $k_{\parallel}$ .** For the kind of intermittent and extremely anisotropic structures seen these simulations, the interpretation of our results in terms of structure functions is complicated. Here we concentrate on  $k_{\parallel}(k_{\perp})$  as a measure of field line curvature. There may be other independent length scales parallel to  $\mathbf{B}_0$  characterizing the properties of the magnetic field structures.

The term  $\mathbf{B} \cdot \nabla \mathbf{B}$  describes magnetic tension and is approximately equal to  $B_0 k_{\parallel} b_l$  for an isolated eddy in a uniform mean field  $\mathbf{B}_0$ . Here  $k_{\parallel} \propto 1/l_{\parallel}$  and  $l_{\parallel}$  is the characteristic length scale parallel to  $\mathbf{B}_0$ , which is known to be larger than the perpendicular length scale. Cho & Vishniac (2000) and Cho, Lazarian & Vishniac (2002) argued that, in actual turbulence, eddies are aligned with the local mean field  $\mathbf{B}_L$ . We can obtain the *local frame representation* of  $k_{\parallel}$ , by considering an eddy lying in the *local* mean field  $\mathbf{B}_L$ :  $\mathbf{B}_L \cdot \nabla \mathbf{b}_l \approx B_L k_{\parallel} b_l$ .<sup>1</sup> Fourier transform of both sides yields  $|\widehat{\mathbf{B}_L \cdot \nabla \mathbf{b}_l}|_{\mathbf{k}} \approx B_L k_{\parallel} |\widehat{b}|_{\mathbf{k}}$ , where hatted variables are Fourier-transformed quantities. From this, we have

$$k_{\parallel} \approx \left( \frac{\sum_{k \leq |\mathbf{k}'| < k+1} |\widehat{\mathbf{B}_L \cdot \nabla \mathbf{b}_l}|_{\mathbf{k}'}^2}{B_L^2 \sum_{k \leq |\mathbf{k}'| < k+1} |\widehat{b}|_{\mathbf{k}'}^2} \right)^{1/2}. \quad (5)$$

Figure 2 shows that by this measure  $k_{\parallel}$  is nearly constant:

$$k_{\parallel} \approx k_{\parallel,d} = \text{constant}, \quad (6)$$

where  $k_{\parallel,d}$  is the parallel wavenumber at the viscous damping scale.<sup>2</sup> In the second-order hyperdiffusion run 384PH2-B01,  $k_{\parallel}$  is almost constant up to  $k \sim 50$ . The sharp rise after  $k \sim 50$  is due to magnetic dissipation and the exponential suppression of the magnetic field energy. The third order hyperdiffusion run (the dotted line) shows more extended range of constant  $k_{\parallel}$  since magnetic dissipation occurs at larger  $k$ 's.

We checked whether or not equation (5) gives a reasonable result for ordinary (i.e. *not* viscously damped) MHD turbulence. Cho & Vishniac (2000) showed numerically that  $k_{\parallel} \propto k_{\perp}^{2/3}$  using structure functions when the turbulence is threaded by a strong external magnetic field (see Goldreich & Sridhar 1995 for a theoretical derivation). When we applied the method in equation (5) to this case we recovered the relation  $k_{\parallel} \propto k_{\perp}^{2/3}$ , confirming our intuitive notion that equation (5) can provide us with a coordinate-independent way of calculating  $k_{\parallel}$  as a function of  $k_{\perp}$ .

**Intermittency.** In Figure 3, we show strength of small scale magnetic fields in a plane perpendicular to the mean field  $\mathbf{B}_0$ . Darker tones represent stronger magnetic fields. We also plot small scale magnetic vectors projected on the plane. We obtain the small scale magnetic

<sup>1</sup>There can be many ways to define the local mean field  $\mathbf{B}_L$ . In this paper, we obtain  $\mathbf{B}_L$  for an eddy of (perpendicular) size  $l \propto 1/k$  by eliminating the Fourier modes whose perpendicular wavenumber is greater than  $k/2$  and  $\mathbf{b}_l$  by eliminating the Fourier modes whose perpendicular wavenumber is less than  $k/2$ .

<sup>2</sup>Constancy of  $k_{\parallel}$  means an extreme form of anisotropy: eddies have a constant parallel size while they can have extremely small perpendicular size.

field by eliminating Fourier modes with  $k < 20$ . Only part of the plane is shown here. We see that the magnetic structures are very intermittent.<sup>3</sup> We also see that the typical radius of curvature of field lines in the plane is much larger than the typical perpendicular scale for field reversal. The typical radius of curvature of field lines corresponds to the viscous damping scale, indicating that stretched structures are results of the shearing motions at the viscous damping scale. This is consistent with Figure 2, which shows that the parallel wavelength at the viscous damping scale is also reflected in the curvature of the small scale field lines. There is no preferred direction for these elongated structures. A similar plot for ordinary (*not* viscously damped) MHD turbulence shows much less intermittent structures.

**What is the Scaling?** In this section, we give a simple set of scaling relations for the properties of this regime (e.g.  $20 < k < 50$  for Run 384PH3-B<sub>0</sub>1). Later, in Lazarian, Vishniac & Cho (2002, henceforth LVC02), we will discuss the physical basis for these scaling relations in detail.

We first note that the magnetic spectrum is roughly proportional to  $k^{-1}$ . When the shearing by the motion at scale  $l_d$  dominates that of the scale  $l$ , the damping-scale shearing timescale ( $l_d/v_d$ ) becomes the characteristic timescale at the scale  $l$ . Note that the characteristic timescale is scale-independent. Assuming a local cascade of energy in phase space we have

$$b_l^2/(l_d/v_d) \approx \text{constant}, \quad (7)$$

so that  $b_l \approx \text{constant}$ , which, in turn, implies

$$E_b(k) \propto k^{-1}. \quad (8)$$

This is identical to the viscous-convective range of a passive scalar in hydrodynamic turbulence (see, for example, Lesieur 1990).

Figure 2 suggests that  $k_{\parallel} \approx \text{constant}$  below the cutoff.

Figure 3 shows that the magnetic structures are very intermittent below the viscous cutoff. Assuming that the filaments are characterized by a rough balance between viscous drag and magnetic tension, calculations in LVC02 predict that

$$E_v(k) \propto k^{-4} \quad (9)$$

which is almost exactly true in our simulations.

<sup>3</sup>This is a real physical effect. When we use a real magnetic diffusivity, we also obtain highly intermittent structures similar to those in Fig. 3.

#### 4. Implications

The intermittent small scale structures that we predict here should have important implications for transport processes (heat, cosmic rays, etc.) in partially ionized plasmas. We also speculate that they might have some relation to the tiny-scale atomic structures (TSAS). Heiles (1997) introduced the term TSAS for the mysterious H I absorbing structures on the scale from thousands to tens of AU, discovered by Deiter, Welch & Romney (1976). Analogs are observed in NaI and CaII (Meyer & Blades 1996; Faison & Goss 2001; Andrews, Meyer & Lauroesch 2001) and in molecular gas (Marscher, Moore & Bania 1993). Recently Deshpande, Dwarakanath & Goss (2000) analyzed channel maps of opacity fluctuations toward Cas A and Cygnus A. They found that the amplitudes of density fluctuations at scales less than 0.1 pc are far larger than expected from extrapolation from larger scales, possibly explaining TSAS. This study, however, cannot answer what confines those presumably overpressured (but very quiescent!) blobs of gas. Deshpande (2000) related those structures to the shallow spectrum of interstellar turbulence.

Figure 1 indicates that while velocity decreases rapidly, but *not* exponentially, below the viscous damping scale, the magnetic field fluctuations persist, thereby providing nonthermal pressure. Magnetic structures perpendicular to the mean magnetic field are compensated by pressure gradients from density fluctuations reminiscent of the Dishpande et al. (2000) observations.

Our calculations are applicable on scales from the viscous damping scale (determined by equating the energy transfer rate with the viscous damping rate;  $\sim 0.1$  pc in the Warm Neutral Medium with  $n = 0.4 \text{ cm}^{-3}$ ,  $T = 6000 \text{ K}$ ) to the ion-neutral decoupling scale (the scale at which viscous drag on ions becomes comparable to the neutral drag;  $\ll 0.1$  pc). Below the viscous scale the fluctuations of magnetic field obey the damped regime shown in Figure 1 and produce density fluctuations. If gas is close to be thermally unstable (Vazquez-Semadeni, Gazol & Scalo 2000), moderate fluctuations of pressure cause substantial density excursions. For typical Cold Neutral Medium gas, the scale of neutral-ion decoupling decreases to  $\sim 70\text{AU}$ , and is less for denser gas. TSAS may be created by strongly nonlinear MHD turbulence!

The issue of an adequate description of turbulence in the newly found regime of persistent turbulence goes much beyond the TSAS formation. The accumulation of energy at small scales is important for problems of cosmic ray transport, magnetic reconnection, and formation of clumps in molecular clouds. We expect to make significant progress in those fundamentally important directions as soon as we describe properly the new regime of MHD turbulence.

## 5. Conclusion

We have considered MHD turbulence with  $\nu \gg \eta$ , which implies that the viscous cutoff occurs at a scale much larger than the magnetic diffusion scale. It has been believed that the damping of the fluid motion is accompanied by the suppression of magnetic structures below the viscous cutoff scale. To the contrary, we have found that the magnetic field can have a rich structure below the viscous cutoff scale. Judging from our (limited) numerical results, we conclude that magnetic field perturbations have a similar power distribution as a passive scalar, despite the obvious importance of magnetic forces. In particular, the spectrum follow a  $k^{-1}$  law. The parallel wavenumber, which is an indicator of the degree of anisotropy, is almost constant. Consequently, the magnetic field has an extreme form of anisotropy. In summary, we have found that

1.  $E_b(k) \propto k^{-1}$ ,
2.  $E_v(k) \propto k^{-4}$ ,
3.  $k_{\parallel} \approx \text{constant}$ .

We discussed the possibility that this small scale magnetic field is the cause of the tiny-scale atomic structure. The small scale magnetic structure will affect many astrophysical processes (e.g. cosmic-ray transport, reconnection, etc) that depend on the statistical properties of MHD turbulence.

J.C. thanks Peter Goldreich for clarifying the idea of calculating  $k_{\parallel}$ . A.L. and J.C. acknowledge the support of NSF Grant AST-0125544. E.V. acknowledges the support of NSF Grant AST-0098615. This work was partially supported by National Computational Science Alliance under AST000010N and utilized the NCSA SGI/CRAY Origin2000.

## REFERENCES

Andrews, S. M., Meyer, D. M., & Lauroesch, J. T. 2001, ApJ, 552, L73  
Armstrong, J. W., Rickett, B. J., & Spangler, S. R. 1995, ApJ, 443, 209  
Cho, J. & Vishniac, E. T. 2000, ApJ, 539, 273  
Cho, J., Lazarian, A., & Vishniac, E. T. 2002a, ApJ, 564, 291  
Deshpande, A.A. 2000, MNRAS, 317, 199

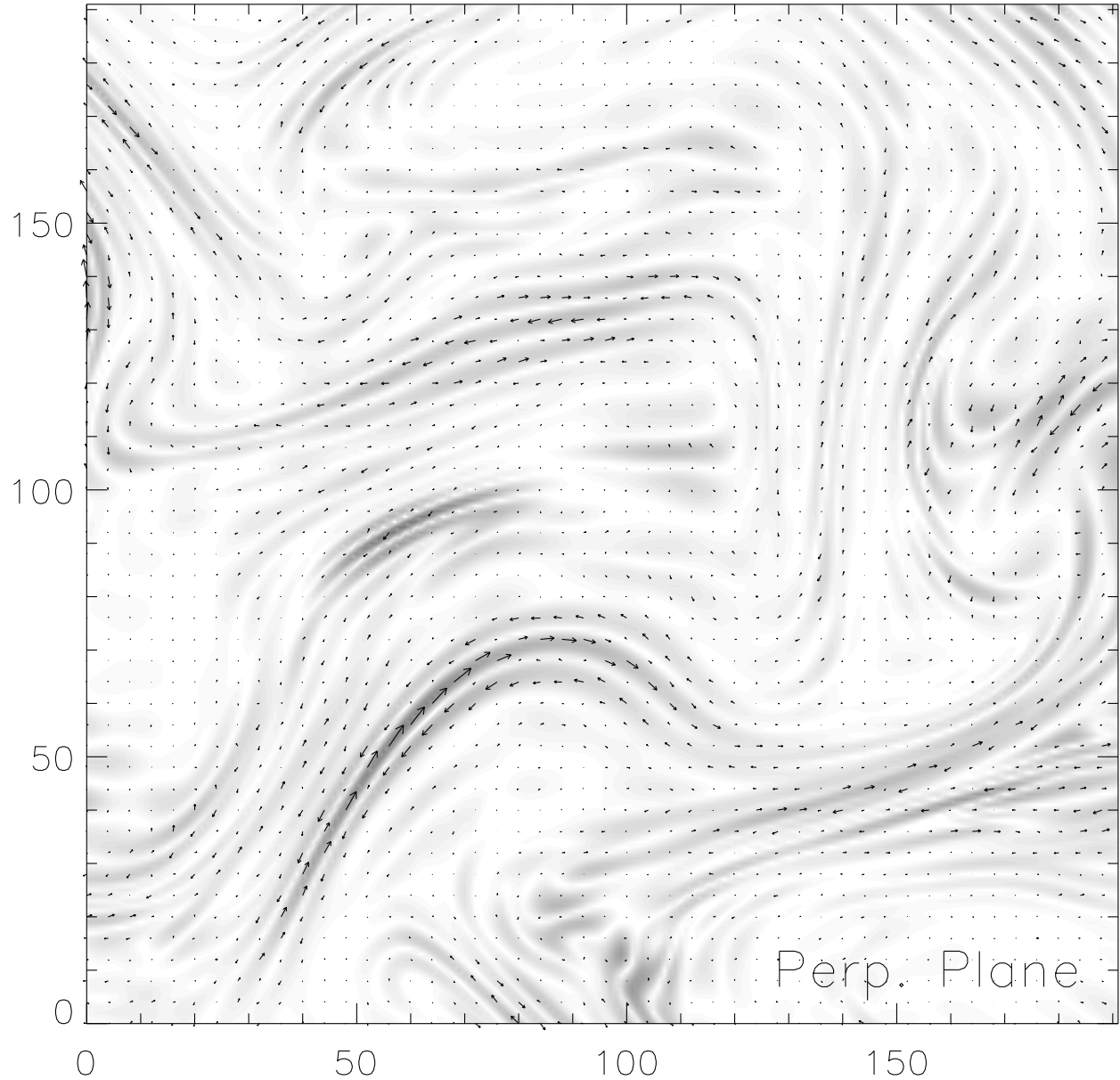


Fig. 3.— Strength of magnetic field in a plane perpendicular to  $\mathbf{B}_0$  at  $t=12$ . Arrows are magnetic fields in the plane. Only 1/4 is shown. Note highly intermittent structures. Run 384PH3-B<sub>0</sub>1.

Deshpande, A.A., Dwarakanath, K.S., Goss, W.M., 2000, ApJ, 543, 227

Dieter, N.H., Welch, W.J., & Romney, J.D. 1976, ApJ, 206, L113

Faison, M.D., Goss, W.M. 2001, AJ, 121, 2706

Goldreich, P. & Sridhar, H. 1995, ApJ, 438, 763

Heiles, C. 1997, ApJ, 481, 193  
Kulsrud, R.M., & Anderson, S.W. 1992, ApJ, 396, 606  
Larson, R. B. 1981, MNRAS, 194, 809  
Lazarian, A.& Vishniac, E. T., & Cho, J. 2002, in preparation (LVC02)  
Lesieur, M. 1990, Turbulence In Fluids (Dordrecht: Kluwer)  
Maron, J. & Cowley, S. 2002, astro-ph/0111008  
Marscher, A.P., Moore, E. M., & Bania, T. M. 1993, 419, L101  
Myers, P.C. 1983, ApJ, 270, 105  
Meyer, D.M., Blades, J.C. 1996, ApJ, 464, L179  
Scalo, J. M. 1984, ApJ, 277, 556  
Stanimirovic, S., & Lazarian, A. 2001, ApJ, 551, L53  
Vazquez-Semadeni, E., Gazol, A., Scalo, J. 2000, ApJ, 540, 271